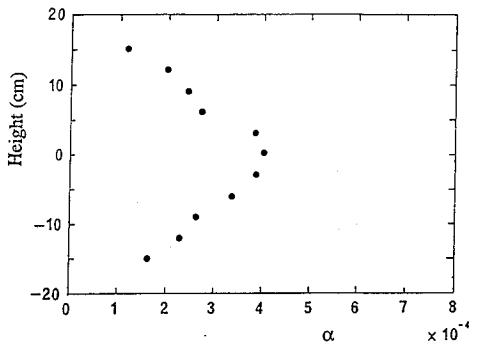

Fig. 6 Radial profile of the ion fraction.

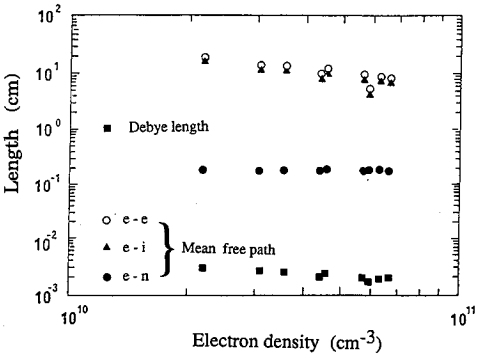

Fig. 7 Characteristic lengths of the plasma as a function of the electron density.

with precedent results by hyperfrequency propagation (2.45–5 GHz) in a boundary layer on a flat plate.

The theory associated with the noncollisional potential sheath is justified if the energy distribution for the electrons is a Maxwellian function, and if the shortest mean free path is much larger than the Debye length. Exponential increase noticed for the current collected by the sensitive part of the probe leads to the assumption of a Maxwellian distribution function for electron energy.

Using the assumption of a thermal local equilibrium between the electron temperature and the translational temperature of heavy species and using the measured static pressure, the ion fraction α of the plasma is evaluated from the relation $\alpha = n_e k T_e / p$. For the measurements made, the ionization fraction is about 10^{-4} (4×10^{-4} on the axis and 10^{-4} at 15 cm from the axis) (Fig. 6). Various mean free paths have been calculated with formulas expressing electron–ion, electron–electron, and electron–neutral collision frequencies:

$$\nu_{e-i}(s^{-1}) = 2.4\ 10^{-5} * n_e(\mathrm{cm}^{-3}) * T_e(eV)$$

$$\nu_{e-e}(s^{-1}) = 0.85 * \nu_{e-i}$$

$$\nu_{e-n}(s^{-1}) = 4\ 10^{9} * p(\mathrm{Torr}) * (T_e(eV))^{1/2}$$

eV: electron-volt.

The electron temperature and electron density show that the Debye length is always much shorter than the electron–neutral mean free path, which is the shortest among the three (Fig. 7). The assumption of a noncollisional path potential sheath is then justified.

The described plasma generator is used to obtain ionized air jets without using an oxygen injection into the plasma either straight in the jet, or close to the neck of the nozzle. The electron characteristics in density and temperature, as well as the pressure and jet stability, make the ionized gas obtained interesting to study for atmospheric re-entry problems. The ionic composition of jets obtained will be analyzed by a quadripolar mass spectrometer.

References

[1]"Technical Evaluation Report on Fluid Dynamics," Panel Symposium on Aerodynamics of Hypersonic Lifting Vehicles, AGARD-AR-246, 1988.

[2]Dunn, M. G., and Lordi, J. A., "Measurement of Electron Temperature and Number Density in Shock-Tunnel Flow," *AIAA Journal,* Vol. 7, No. 11, 1969, pp. 2099–2104.

[3]Lederman, S., Bloom, M. H., and Widhopf, G. F., Experiments on Cylindrical Electrostatic Probes in a Slightly Ionized Hypersonic Flow," *AIAA Journal,* Vol. 6, No. 11, 1968, 2133–2139.

[4]Scharfman, W. E., and Bredfeldt, H. R., "Experimental Investigation of Flush-Mounted Electrostatic Probes," *AIAA Journal,* Vol. 8, No. 4, 1970, pp. 662–665.

[5]Thompson, W. P., and de Boer, P. C. T., "Ion Density Measurements with an Electric Probe," *AIAA Journal,* Vol. 13, No. 8, 1975, pp. 1115–1117.

[6]Dorman, F. H., and Hamilton, J. A., "Double Probes in a Slightly Ionized Collisional Plasma," *International Journal of Mass Spectrometry and Ion Physics,* Vol. 20, No. 4, 1976, pp. 411–424.

[7]Blackwell, H. E., Yuen, E., Arepalli, S., and Scott, C. D., "Nonequilibrium Shock Layer Temperature Profiles from Arc Jet Radiation Measurements," AIAA Paper 89-1679, Buffalo, NY, June 1989.

[8]Starner, K. E., "Evaluation of Electron Quench Additives in a Subsonic Air Arc Channel," *AIAA Journal,* Vol. 7, No. 12, 1969, pp. 2357–2358.

[9]Lasgorceix, P., Dudeck, M. A., Caressa, J. P., "Measurements in Low Pressure, High Temperature and Reaction Nitrogen Jets," AIAA Paper 89-1919, Buffalo, NY, June 1989.

[10]Messerschmid, E., "Characterization of IRS Plasma Jet," Hermès Plasma Diagnostics Meetings, Stuttgart, RFA, Nov. 25, 1987.

Radiative Transfer in Multidimensional Enclosures with Specularly Reflecting Walls

A. S. Jamaluddin* and W. A. Fiveland†
Babcock & Wilcox, Alliance, Ohio 44601

Introduction

RADIATION is the dominant heat transfer mechanism in most large-scale industrial applications. The efficiency of radiative transfer depends on the boundary conditions, e.g., the temperature and the emissivity of the surrounding walls, and the target where heat transfer is desired. Previous studies[1–3] have shown that radiative transfer is highly sensitive to the wall emissivity.

In most heat transfer calculations, the walls are assumed to be diffusely reflecting. In some practical applications, however, the wall reflectivity may be partially specular. Industrial furnaces used for drying paint are an example of furnaces with partially specular walls.

The present work studies the effect of a specular component of reflectivity on wall radiative flux. The reflectivities, defined as $(1 - \epsilon)$ for an opaque surface, are segmented into diffuse and specular components, and the S_n discrete-ordinates method is employed to obtain solutions of the radiative transfer equation. An S_4 approximation is used, since higher order ap-

Presented at the AIAA/ASME 5th Joint Heat Transfer Conference, Seattle, WA, June 18–20, 1990; received June 25, 1990; revision received Jan. 24, 1991; accepted for publication Jan. 24, 1991.

*Senior Research Engineer, Alliance Research Center; currently, with Shell Development Co., P.O. Box 1380, Houston, TX 77251-1380.

†Group Supervisor, Alliance Research Center.

proximations did not substantially improve the results. The results are compared with those for purely diffuse wall reflectivity, which were shown[2-6] to be accurate, to quantify the effect of a specular component of reflectivity at the walls.

Analysis

The radiative transfer equation for three-dimensional rectangular enclosures may be written as[2]

$$\mu_m \frac{\partial I_m}{\partial x} + \eta_m \frac{\partial I_m}{\partial y} + \xi_m \frac{\partial I_m}{\partial z} = -(k_a + k_s)I_m + k_a I_b + \frac{k_s}{4\pi}\int_{4\pi} P(\Omega,\Omega')I_{m'}\, d\Omega' \quad (1)$$

where I_m is the intensity in the discrete direction m; μ_m, η_m, and ξ_m are the direction cosines for the direction Ω; x, y, and z are the distances along the coordinate axes; k_a, k_s, and I_b are the absorption and scattering coefficients, and black-body radiative intensity of the medium; and $P(\Omega,\Omega')$ is the phase function. If the reflectivity at the walls has diffuse and specular components, the boundary conditions for Eq. (1) are[6]

at $x = 0$

$$I_m^+ = \epsilon_w I_{bw} + f_d(1-\epsilon_w)\frac{q_x^-}{\pi} + (1-f_d)(1-\epsilon_w)I_{m-}; \quad \mu_m > 0 \quad (2)$$

at $x = L$:

$$I_m^- = \epsilon_w I_{bw} + f_d(1-\epsilon_w)\frac{q_x^-}{\pi} + (1-f_d)(1-\epsilon_w)I_{m-}; \quad \mu_m < 0 \quad (3)$$

at $y = 0$:

$$I_m^+ = \epsilon_w I_{bw} + f_d(1-\epsilon_w)\frac{q_y^-}{\pi} + (1-f_d)(1-\epsilon_w)I_{m-}; \quad \eta_m > 0 \quad (4)$$

at $y = W$:

$$I_m^- = \epsilon_w I_{bw} + f_d(1-\epsilon_w)\frac{q_y^+}{\pi} + (1-f_d)(1-\epsilon_w)I_{m-}; \quad \eta_m < 0 \quad (5)$$

at $z = 0$:

$$I_m^+ = \epsilon_w I_{bw} + f_d(1-\epsilon_w)\frac{q_z^-}{\pi} + (1-f_d)(1-\epsilon_w)I_{m-}; \quad \xi_m > 0 \quad (6)$$

at $z = H$:

$$I_m^- = \epsilon_w I_{bw} + f_d(1-\epsilon_w)\frac{q_z^+}{\pi} + (1-f_d)(1-\epsilon_w)I_{m-}; \quad \xi_m < 0 \quad (7)$$

In Eqs. (2–7), L, W, and H represent the length, width, and height of the enclosure, ϵ_w and I_{bw} are the emissivity and the black-body radiative intensity of the wall, $q_n^{\pm}$ is the incident radiative flux, and f_d is the fraction of the reflectivity which is diffuse. + and − represent the positive and negative direction of propagation. I_m refers to the directional intensity which is the mirror image of the intensity for which the equation is written. A total of 24 such directions are considered in an S_4 solution.

The ordinates, quadrature weights, details of formulation, and solution scheme are reported in Refs. 2 and 3.

Results

Parametric Sensitivity

A square cavity containing a radiatively gray, isotropically scattering medium with an optical thickness of 1.0 (which has been studied earlier by various investigators[2,4,7]) is considered, with the difference that the wall emissivity is assumed to be 0.5 rather than 1.0 as done in those studies. The pre-

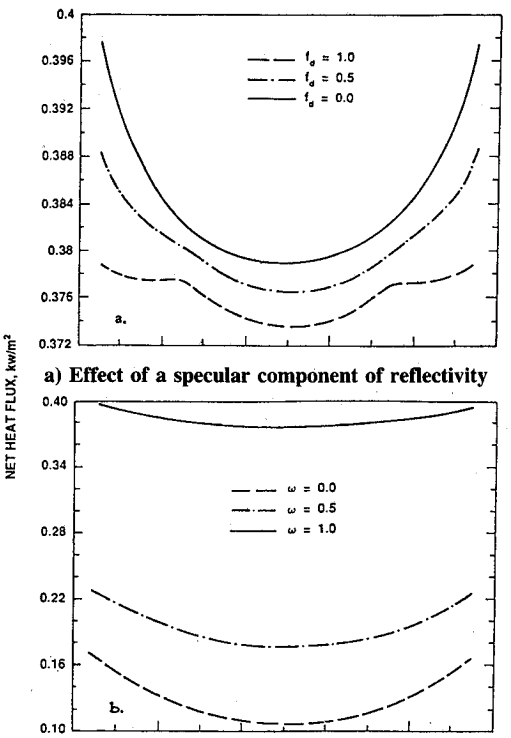

a) Effect of a specular component of reflectivity

b) Effect of the albedo of scatter

Fig. 1 Predicted net radiative fluxes at the hot wall of a square cavity containing a purely scattering medium: $k_s = 1.0$; $\epsilon_w = 0.5$.

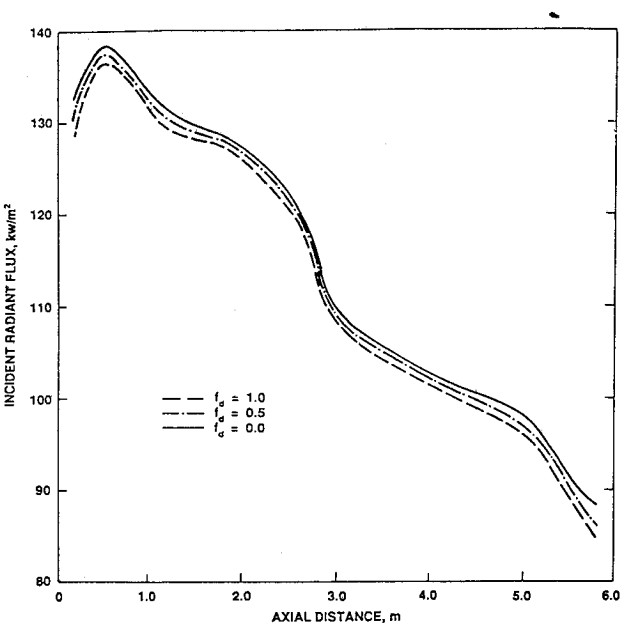

Fig. 2 Effect of a specular component of reflectivity on the predicted incident radiant fluxes to the floor of the IFRF furnace.

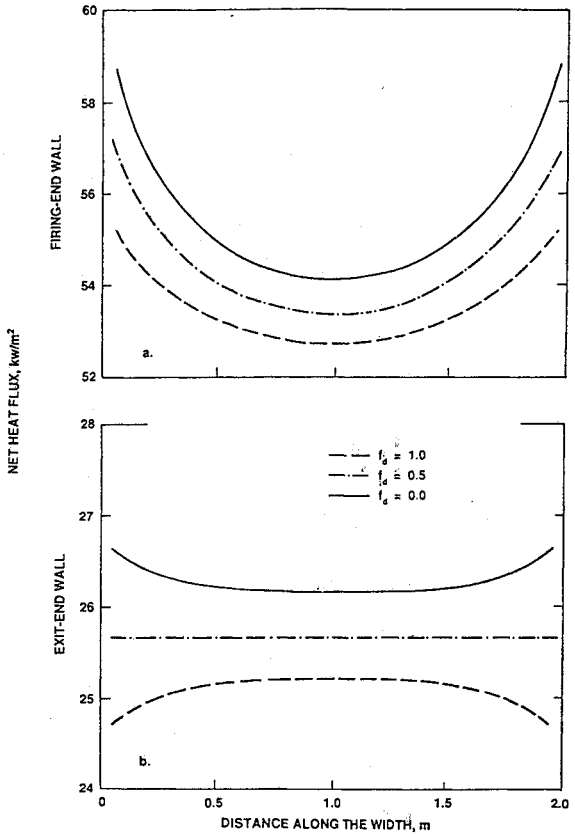

Fig. 3 Effect of a specular component of reflectivity on the net radiative fluxes to the firing and exit end walls of a rectangular enclosure containing a scattering medium.

dicted wall heat fluxes for purely specular wall reflection were found to be grid-independent for grid sizes varying between 5×5 and 15×15, and therefore a 10×10 grid was chosen for the results presented here. Also, the predicted radiative fluxes varied by no more than ~1.0% anywhere in the enclosure as the order of discrete-ordinates approximation was varied between S_2 and S_6. The wall heat flux proportionally increases with increasing wall emissivity, as expected.

Figure 1a shows the predicted wall fluxes with f_d of 1.0, 0.5, and 0.0. The heat flux is little affected near the center of the wall (<2% difference at $x/L = 0.5$), and up to 5.5% at the edges. An increase in specular reflectivity (i.e., a decrease in f_d) causes an upward shift in the wall heat flux profile. As the scattering albedo is increased, the net wall heat flux for an enclosure with specular reflection at the walls ($\epsilon_w = 0.5$) also increases (see Fig. 1b). The medium scatters isotropically, with an emissive power of unity. The net heat flux at the hot wall increases nearly three times as the albedo increases from 0.0 to 1.0. This effect, however, is case dependent; if the medium were at a higher temperature compared to the hot wall, the net heat flux to the cold walls would decrease with increasing albedo of scatter.

Three-Dimensional Enclosure with Nonscattering Medium

The geometry and the conditions for the 3-D nonscattering system pertain to the International Flame Research Foundation (IFRF) M3 trials (Flame 10), and are described in Ref. 8. For this furnace, the floor may be viewed as the target where the transfer of heat is desired. The incident radiant fluxes on the furnace floor with f_d of 0.5 and 0.0 are compared with those for diffuse wall reflection ($f_d = 1.0$) in Fig. 2. The predicted fluxes for diffuse wall reflection were shown[2] to be in excellent agreement with the zone model predictions.[8] The figure shows that increasing the specular component of reflection enhances the local fluxes, while the heat flux profile retains its shape. The overall heat transfer to the floor (target) is increased by nearly 1.0% for the 50% specular, and by about 2% for the purely specular reflection at the walls.

Three-Dimensional Enclosure with Scattering Medium

An idealized enclosure studied in Refs. 2, 5, and 9 is modeled. The geometry and the boundary conditions are described in Ref. 9. Figure 3 shows the net wall heat flux at the firing and exit ends. The heat fluxes are plotted using the coordinate along the width of the enclosure, for three wall conditions: diffuse reflection ($f_d = 1.0$), partially specular reflection ($f_d = 0.5$), and purely specular reflection ($f_d = 0.0$). With the wall reflectivity assumed specular, the net heat flux is 3–4% higher at the center, and about 7–8% higher at the edges, as compared to the heat fluxes under diffuse wall conditions. These enhancements in heat transfer are due to the specularity alone, since the medium temperature remains practically unaltered as f_d is varied between 0.0 and 1.0.

Conclusion

The results presented in this paper indicate that the presence of a specular component of reflection at the walls enhances heat transfer in two- and three-dimensional rectangular enclosures. This finding is supported by industrial applications where highly reflective walls are used to improve performance. The present work also demonstrates that the discrete-ordinates method can be applied to predicting radiative transfer in multidimensional enclosures where the walls reflect specularly.

Acknowledgment

A. S. Jamaluddin wishes to thank Karen Rhoden of Shell Development Company for helping prepare the manuscript.

References

[1]Menguc, M. P., and Viskanta, R., "A Sensitivity Analysis for Radiative Heat Transfer in a Pulverized Coal-Fired Furnace," *Combustion Science and Technology*, Vol. 51, 1987, pp. 51–74.

[2]Jamaluddin, A. S., and Smith, P. J., "Predicting Radiative Transfer in Rectangular Enclosures Using the Discrete-Ordinates Method," *Combustion Science and Technology*, Vol. 59, 1988, pp. 321–340.

[3]Jamaluddin, A. S., and Smith, P. J., "Predicting Radiative Transfer in Axisymmetric Cylindrical Enclosures Using the Discrete-Ordinates Method," *Combustion Science and Technology*, Vol. 62, 1988, pp. 173–186.

[4]Fiveland, W. A., "Discrete-Ordinates Solutions of the Radiative Transport Equation for Rectangular Enclosures," *Journal of Heat Transfer*, Vol. 106, 1984, pp. 699–706.

[5]Fiveland, W. A., "Three-Dimensional Radiative Heat Transfer Solutions by the Discrete-Ordinates Method," *Journal of Thermophysics and Heat Transfer*, Vol. 2, 1988, pp. 309–316.

[6]Jamaluddin, A. S., and Fiveland, W. A., "Radiative Transfer in Multi-Dimensional Enclosures with Specularly Reflecting Walls," *Proceedings of 1990 National Heat Transfer Conference*, Seattle, WA, June 1990.

[7]Ratzel, A. C., and Howell, J. R., "Two-Dimensional Radiation in Absorbing-Emitting-Scattering Media Using the P-N Approximation," ASME Paper 82-HT-19, 1982.

[8]Hyde, D. J., and Truelove, J. S., "The Discrete-Ordinates Approximation for Multi-Dimensional Radiant Heat Transfer in Furnaces," AERE R-8502, AERE Harwell, U.K., 1977.

[9]Menguc, M. P., and Viskanta, R., "Radiative Transfer in Three-Dimensional Rectangular Enclosures Containing Inhomogeneous Anisotropically Scattering Media," *Journal of Quantitative Spectroscopy & Radiative Transfer*, Vol. 33, 1985, pp. 533–549.